Interplay of adsorption and surface mobility in tracer diffusion in porous media

Carlos Olivares[*] and F. D. A. Aarão Reis[†]
Instituto de Física, Universidade Federal Fluminense, Avenida Litorânea s/n, Niterói, Rio de Janeiro 24210-340, Brazil

(Received 13 March 2019; published 15 August 2019)

We model the diffusion of a tracer that interacts with the internal surface of a porous medium formed by a packing of solid spheres. The tracer executes a lattice random walk in which hops from surface to bulk sites and hops on the surface have small probabilities compared to hops from bulk sites; those probabilities are related to bulk and surface diffusion coefficients and to a desorption rate. A scaling approach distinguishes three regimes of steady state diffusion, which are confirmed by numerical simulations. If the product of desorption rate and sphere diameter is large, dominant bulk residence is observed and the diffusion coefficient is close to the bulk value. If that product is small and the surface mobility is low, the tracers are adsorbed most of the time but most hops are executed in the bulk. However, for high surface mobility, there is a nontrivial regime of dominant surface displacement, since the connectivity of solid walls allows the tracers to migrate to long distances while they are adsorbed. In this regime, we observe rounded tracer paths on the sphere walls, which are qualitatively similar to those of a recent experiment on polystyrene particle diffusion. The calculated average residence times are proportional to the bulk and surface densities of an equilibrium ensemble of noninteracting tracers, and the relation between those densities sets the adsorption isotherm. Simulations performed with initially uniform (nonequilibrium) distribution of tracers in the pores show other nontrivial results in cases of dominant surface residence: slow increase of the mean-square displacement at short times, since the tracer has not explored a homogeneous medium, and a remarkable slowdown between the first encounter with a solid wall and the first hop from that point. Relations between our results and other models of diffusion and adsorption in porous media are discussed.

DOI: 10.1103/PhysRevE.100.022120

I. INTRODUCTION

Diffusion of tracers in disordered media has attracted much attention in recent decades due to a large number of technological applications and a large variety of scaling scenarios in experiments and models [1,2]. In a homogeneous medium, normal or Fickean diffusion is characterized by a linear time increase of its mean square displacement, i.e.,

$$\langle r^2 \rangle \approx 2dDt, \tag{1}$$

where D is the diffusion coefficient and d is the dimension of the medium.

Periodic or random packings of solid spheres are models of porous media in which diffusion was already studied theoretically and experimentally [3–10]. Despite the apparently simple features of these packings, nontrivial phenomena may be observed. Kim and Torquato [3,4] calculated the diffusion coefficient as a function of the diameter of a tracer that randomly moved in the interstices of those media and proposed to use that result to describe macromolecule transport in porous media. Kluijtmans and Phillipse [6] measured the diffusion coefficients of fluorescent molecules and of colloidal particles in media with that geometry and obtained values much smaller than the theoretical predictions, but explained the discrepancies by hydrodynamic interactions. In Refs. [5,9], the diffusion coefficient was calculated in models with different diffusivities in the bulk pores and on the surfaces of the spheres. Recently, Babayekhorasani *et al.* [8] studied diffusion of colloidal particles in the interstices of a random packing of glass beads and, depending on the choice of the solvent, obtained a normal behavior as in Eq. (1) or subdiffusive behavior [1].

Here we study a model of tracer diffusion in periodic porous media formed between solid spheres considering that the diffusions along the solid walls and in the bulk fluid have different coefficients and that desorption from those walls has a low rate compared to the adsorption. These features are represented in a random walk model by different probabilities of hops in the bulk and along the walls and different probabilities for adsorption and desorption. Instead of focusing on a particular application, our aim is to analyze the scaling scenario that results from the interplay of adsorption, bulk mobility, and surface mobility.

A phenomenological approach is developed to distinguish cases of dominant bulk residence and dominant surface residence and, in the latter case, to distinguish the regimes of dominant bulk or surface displacement. The diffusion coefficients in these scaling regimes are determined in terms of the stochastic parameters of the model and the ratio R between solid sphere radius and tracer diameter; these parameters can be in turn expressed in terms of kinetic parameters, namely the surface and bulk diffusion coefficients and a desorption rate. Numerical simulations confirm the predictions of the scaling approach. Our discussion will highlight the nontrivial

[*]carlosolivares@id.uff.br
[†]reis@if.uff.br

features of the regime of dominant surface residence and displacement, in which the tracers move to long distances while they are adsorbed at the solid walls. For instance, the rounded trajectories shown in the simulations are qualitatively similar to those observed in experiments with colloidal particles [8]. We also address the problem of an ensemble of noninteracting tracers with the same kinetic parameters. At long times, their densities in the bulk and on the solid surface are proportional to the corresponding residence times of a single tracer, and the relation between those densities is the adsorption isotherm of the system.

Our simulations are performed with an initial uniform distribution of tracers in the pore space. This is a non-equilibrium condition which leads to nontrivial properties at short times, before the asymptotic scaling is attained. For small rates of desorption and surface diffusion, we show a remarkable slow down of diffusion when the average displacement is of order $\lesssim R$, which is quantitatively explained by an extended scaling approach. At shorter times, when the tracers have explored only small regions between the spheres, the mean square displacement increases slower than linearly in time.

This paper is organized as follows. In Sec. II, we present the model and the methods of solution. In Sec. III, we present numerical results for several parameter sets to show the possible time evolutions of the mean square displacement and tracer trajectories. In Sec. IV, the diffusion coefficient is predicted in the three scaling regimes and the scaling relations are checked numerically. In Sec. V, the equilibrium isotherm for an ensemble of tracers is obtained. In Sec. VI, we analyze the slowdown observed in simulations with initial uniform distribution of tracers and the crossover to normal diffusion. In Sec. VII, we discuss relations with other models. In Sec. VIII we present our conclusions.

II. MODEL AND METHODS

A. Model definition

Our model is defined in a simple cubic lattice in which the edge of a site is a. The solid part of the medium is formed by discretized spheres of radius aR whose centers are organized in a simple cubic lattice of edge $2aR$, with integer R, as illustrated in Fig. 1(a). In this geometry, neighboring spheres have a small contact region. We assume that the porous medium between the spheres is filled with a fluid. The porosity of this medium in the continuous limit (sufficiently large spheres) is ≈ 0.4764; for $R \sim 10$, the porosity is not very different from this value.

The neighborhood of a site is defined as the set of 6 nearest neighbor (NN) and 12 next nearest neighbor (NNN) sites. This 18-site neighborhood was considered in previous models because if simplifies the description of adsorbed particle diffusion [11]. The pore sites that have no neighboring solid site are called bulk sites. The pore sites that have one or more neighboring solid sites are called surface sites. These definitions are illustrated in Fig. 1(b).

The tracers do not interact with each other, which may be a reasonable assumption for a dilute solution. Each tracer occupies a single pore site, as shown in Fig. 1(b), and its diffusion is represented by a random walk in the pore sites. A tracer is in the adsorbed state if it is at a surface site.

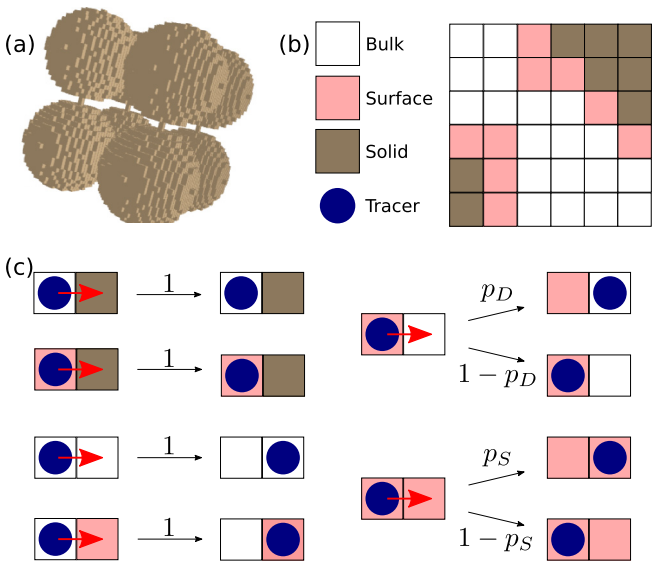

FIG. 1. (a) Spheres of radius $R = 10$. (b) The three types of sites, whose spatial organization is illustrated in a square region. A tracer can occupy a bulk or a surface site. (c) Hop attempts of the tracer are indicated by red arrows. Black arrows show the possible outcomes of those attempts with the corresponding probabilities.

In each time interval τ, the tracer attempts to hop to a randomly chosen neighboring site (target site): a NN site is chosen with probability $1/12$ and a NNN is chosen with probability $1/24$; in steady state diffusion, this corresponds to an isotropic discretization of $\nabla^2 P = 0$ for the tracer concentration P [12].

If the current site of the tracer is a bulk site, the hop attempt to any target site (bulk or surface) is accepted with probability 1. If the current site is on the surface, we distinguish three cases. First, a hop attempt to a neighboring solid site is always rejected. Second, a hop to another surface site represents surface diffusion and is executed with probability p_S; otherwise, the hop attempt is rejected and the tracer remains at its current position. Third, a hop to a bulk site represents desorption and is executed with probability p_D; otherwise, the hop attempt is also rejected and the tracer remains at its current position. These possibilities are illustrated in Fig. 1(c).

The tracer displacement along a solid wall may be hindered by hydrodynamic interactions, as discussed in Refs. [8,13–15] in the context of colloidal particle diffusion. Our model proposes a simple stochastic description of the consequences of these interactions by considering $p_S < 1$. Desorption occurs with an increase in the distance between the tracer particle and the solid wall, which also depends on the interaction between the tracer and fluid layers near the wall. Considering an attractive interaction with the wall, we use $p_D < 1$.

We denote as t_D the time of tracer diffusion. A dimensionless diffusion time is defined as

$$t \equiv \frac{t_D}{\tau}. \tag{2}$$

B. Physical interpretation of the model parameters

The lattice constant a may be interpreted as the mean free path of a tracer. Although the illustrations in Figs. 1(b) and 1(c) suggest that the tracer diameter is close to a, the model may also be used for tracers with diameters smaller than a.

If the diffusion coefficient of a tracer in a free solution is D_0 (i.e., a solution in a vessel without obstacles), then this coefficient is related to the time for one hop attempt and to the lattice constant as

$$D_0 = \frac{a^2}{4\tau}. \tag{3}$$

The factor 4 in Eq. (3) is a consequence of the possible hops to NN or NNN sites [11]; with hops only to NNs, that factor would be 6.

The diameter of the solid spheres (obstacles of the porous medium) is

$$d = 2Ra, \tag{4}$$

Consequently, R is the ratio between the sphere radius and the tracer mean free path.

The distinction between bulk and surface sites is necessary for the description of an adsorption process. The assumption that surface sites are only those neighbors of solid sites means that the interaction between the tracer, the solid walls, and the fluid near the walls has a range of the same order as a. This assumption is implicit in several lattice models of colloidal particle adsorption with surface diffusion [16,17]. It also gives reasonable results for growth of macromolecule films and colloidal films [18].

When the tracer is at a bulk site, we assume that the hops to neighboring bulk and surface sites have the same probability (1). Since the hop to a surface site represents a transition to an adsorbed state, our assumption means that the energy barrier for adsorption is neglected. This approximation is also considered in several models of colloidal particle adsorption [16,17].

The reduced probability p_S of hops along the surface of the spheres implies that the surface diffusion coefficient is

$$D_S \sim p_S D_0 \sim \frac{a^2 p_S}{4\tau}. \tag{5}$$

The rate of desorption of a tracer from the surface is

$$r_D \sim \frac{p_D}{\tau}. \tag{6}$$

Our model obeys detailed balance conditions. We associate energies E_B and E_S with bulk and surface sites, respectively, so that the ratio of surface-to-bulk and bulk-to-surface hop probabilities is

$$p_D = \exp\left[(E_S - E_B)/(k_B T)\right]. \tag{7}$$

D_0 and D_S may also be written in terms of activation energies for diffusion and in terms of a characteristic frequency for those hops.

C. Methods of solution

A simple analytical calculation of the diffusion coefficient is not possible for this model because the hopping rates depend not only on the current site but also on the target site; for instance, a surface-to-bulk hop and a surface-to-surface hop have different probabilities. This justifies the use of other methods, namely a combination of scaling arguments and numerical simulations.

The scaling regimes of the model and the crossovers between them are first obtained by an approach which is based on the comparison of characteristic times for diffusion in surface and bulk regions and characteristic lengths of the tracer displacement in those regions. The methods are similar to those used to distinguish scaling regimes in island coarsening with diffusion, aggregation, and detachment [19,20]. Their advantage is the phenomenological description of the interplay between the physical and chemical processes and the system geometry, which helps the extensions to other problems with the same processes.

We also perform simulations of the random walk model in lattices built with spheres of radius R varying from 10 to 320. For $R = 10$, we consider several values of p_S and p_D from 10^{-6} to 10^{-1}; for larger sphere radii, most simulations consider p_D ranging from 10^{-6} to 10^{-2} and $p_S \gg p_D$. For each set of parameters $\{p_S, p_D, R\}$, we calculate the mean square displacement $\langle r^2 \rangle$ by averaging over the trajectories of 10^6 tracers. The maximal hopping times range from $10^6\tau$ to $10^7\tau$.

The initial tracer position in the simulations is randomly chosen among the pore sites. This is not the equilibrium distribution of the tracers. The equilibrium distribution in bulk and surface sites is obtained after long simulation times and is analytically calculated in Sec. IV A.

A dimensionless mean square displacement is defined as

$$r_2(t) \equiv \frac{\langle r^2 \rangle}{a^2}. \tag{8}$$

Thus, ${r_2}^{1/2}$ is an estimate of the effective tracer displacement in lattice units.

The numerical method used here reproduces directly the model rules: at each time interval τ, one NN of the current site is chosen and the hop is executed with the corresponding probability. This is possible in a reasonable computational time because the model is simple and the asymptotic scaling is attained with displacements not much larger than Ra. On the other hand, a kinetic Monte Carlo approach would be necessary in highly inhomogeneous environments, in systems with interactions between the diffusing tracers [19,20], or if chemical reactions were involved [21].

III. OVERVIEW OF SIMULATION RESULTS

Figure 2(a) shows the time evolution of the normalized mean square displacement r_2 in a medium where $R = 10$, for $p_S = 10^{-3}$ [fixed surface diffusion coefficient; Eq. (5)], and for several values of the desorption probability p_D. Figure 2(b) shows the time evolution of the dimensionless mean square displacement r_2 in a medium with $R = 40$, for $p_D = 10^{-3}$ [fixed desorption rate; Eq. (6)], and several values of p_S. These plots contain data for several orders of the ratio p_S/p_D, with two values of the sphere radius.

At long times, the slopes of all plots are close to 1, which is consistent with normal diffusion. This occurs when the

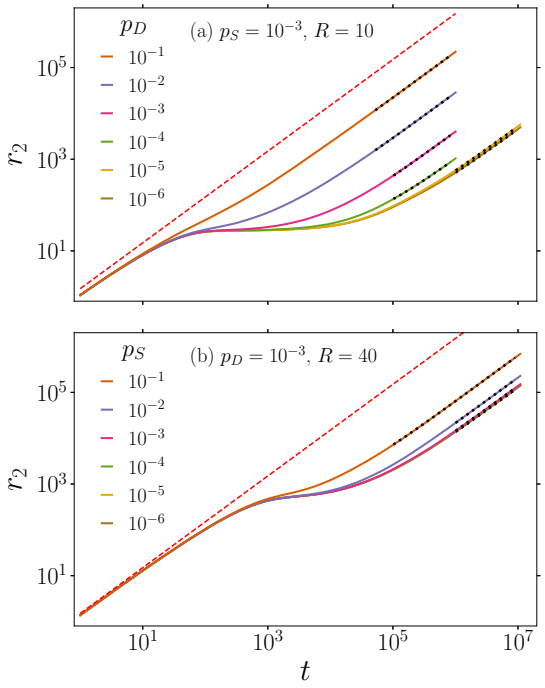

FIG. 2. Mean square displacement as a function of time (solid lines) for the parameters shown in the plots: (a) constant surface diffusion coefficient (decreasing p_D from top to bottom); (b) constant desorption rate (decreasing p_S from top to bottom). Curves for $p_D \leqslant 10^{-5}$ in (a) and for $p_S \leqslant 10^{-3}$ in (b) are superimposed. The red dashed lines have slope 1. The black dotted lines are linear fits of long time data which are used to estimate the diffusion coefficient.

tracer scans a region much larger than the sphere diameter, i.e., $r_2 \gg R^2$. However, in some cases normal diffusion can be observed for r_2 slightly larger than R^2. This is a consequence of the large-scale homogeneity of the medium. The diffusion coefficient is estimated in this long-time regime. It will be predicted by a scaling approach in Sec. IV A and a comparison with the numerical values will be presented in Sec. IV B.

At short times, for small p_D or small p_S, Figs. 2(a) and 2(b) show slopes slightly smaller than 1. Figure 3 highlights this

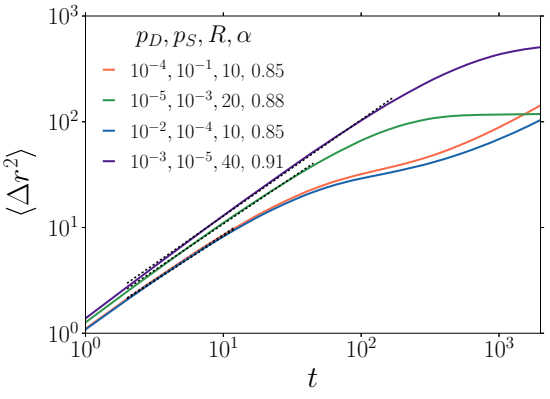

FIG. 3. Mean square displacement as a function of time (from bottom to top at short times, $p_D = 10^{-3}$, 10^{-5}, 10^{-4}, and 10^{-2}). The black dotted lines are linear fits between $r_2 \approx 1$ and $r_2 \approx 0.1R^2$, and the corresponding slopes α are shown.

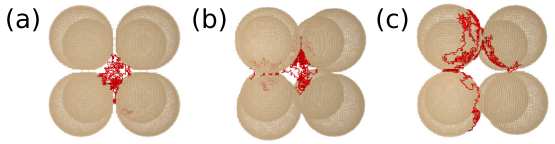

FIG. 4. Examples of tracer trajectories: (a) $p_D = 0.2$, $p_S = 10^{-4}$, $R = 20$, dominant bulk residence; (b) $p_D = 10^{-3}$, $p_S = 10^{-4}$, $R = 20$, dominant surface residence with dominant bulk displacement; (c) $p_D = 10^{-3}$, $p_S = 10^{-1}$, $R = 20$, dominant surface residence and dominant surface displacement. The perspective shows larger transparent spheres in the front and smaller opaque spheres in the back.

short-time scaling of r_2 for four sets of parameters and shows fits of each data set between $r_2 \approx 1$ (average displacement of one particle diameter) and $r_2 \approx 0.1R^2$ (average displacement nearly one third of the radius of the solid spheres). The slopes α of those fits range between 0.85 and 0.91; these values are strongly dependent on the choice of the fitting region, but local slopes are always smaller than 1 in all the fitted ranges.

The slow increase of r_2 compared to the normal diffusion relation [Eq. (1)] is a consequence of the tracer motion in an apparently inhomogeneous medium at short times. In highly disordered media (e.g., fractal media), deviations from this linear relation appear at all timescales [1], which characterizes subdiffusion:

$$\langle r^2 \rangle \sim t^{\alpha}, \tag{9}$$

with $\alpha < 1$; for recent reviews, see Refs. [22,23]. In this context, our results at very short times suggest an apparent (not true) subdiffusion, which shows that the interpretation of short-time results in related models and experiments must be done carefully. Alternatively, our results may also be interpreted in terms of a time varying diffusion exponent, as suggested in Ref. [24], but such an approach is not considered here.

Another nontrivial feature observed in Figs. 2(a) and 2(b) for small p_D and p_S is the plateau of r_2 between the initial regime and the asymptotic regime of normal diffusion. It is typically observed with $r_2 \sim (0.2\text{–}0.3)R^2$, which means that the tracer is confined to a small region for a long time. This localization may last several time decades, as illustrated by the results for $p_D \leqslant 10^{-5}$ in Fig. 2(a).

The confinement is a consequence of the uniform initial distribution of the tracers combined with the strong adsorption after the first collisions with the solid walls. It will be explained by a crossover scaling approach in Sec. VI. Note that this feature differs from the long-time (asymptotic) saturation of the mean square displacement of tracers confined to closed regions, which is observed in porous media below the percolation threshold [1] and which was recently illustrated in models of colloidal particle diffusion in gels [25]. Instead, in the present model, the confinement is always a transient effect.

Figure 4 shows three types of trajectories observed in the simulations. They correspond to the three scaling regimes which will be described in Sec. IV A. In (a), the tracer moves most of the time in the middle of a pore, with rapid collisions with the solid walls. The trajectory in (b) does not have many differences from that in (a), since most hops are executed in

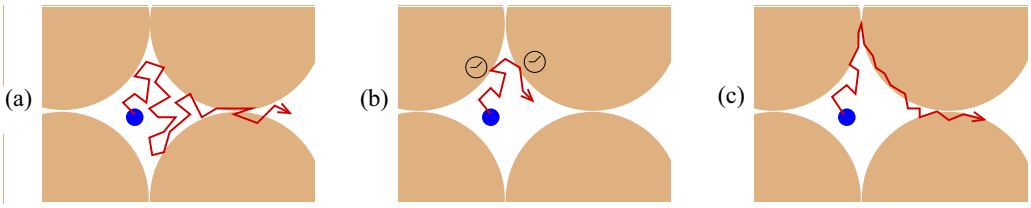

FIG. 5. Three possible diffusion regimes: (a) dominant bulk residence; (b) dominant surface residence with dominant bulk displacement; (c) dominant surface residence and dominant surface displacement.

the middle of the pores (p_S is very small); however, the tracer spends much longer times at the collision points because p_D is small. In (c), the rounded parts of the trajectory shows that most hops of the tracer are executed along the solid walls; a larger value of p_S permits those hops before the tracer desorbs from the wall (p_D is very small).

Rounded trajectories of tracers were also observed in experiments on colloidal particle diffusion in Ref. [8]. The qualitative relation with that work is discussed in Sec. VII.

IV. DIFFUSION COEFFICIENTS

Here we are concerned with the long-time features of the model. We estimate average residence times and diffusion lengths in the surface and in the bulk regions and then present a scaling approach to estimate the order of magnitude of the diffusion coefficient. Numerical results supporting our predictions are presented.

A. Scaling approach

The fraction of the time in which a tracer is at bulk sites is denoted as f_B; the fraction of time at surface sites is denoted as f_S, with $f_B + f_S = 1$. Each fraction is proportional to the product between the hop probability to that set of sites and the density of sites in that sets; see, for instance, a discussion for a broad range of diffusion models in Ref. [26]. The hop probability from bulk to surface is 1 and from surface to bulk is p_D. The densities of surface and bulk sites are defined as ρ_S and ρ_B, respectively, and can be calculated by assuming perfect solid spheres:

$$\rho_S \approx \frac{4\pi R^2}{(2R)^3 - 4\pi R^3/3} = \frac{1}{(2/\pi - 1/3)R},$$
$$\rho_B = 1 - \rho_S \approx 1 - \frac{1}{(2/\pi - 1/3)R}. \tag{10}$$

Consequently, the fractions of the time at the surface and at the bulk are

$$f_S = \frac{\rho_S}{\rho_S + p_D \cdot \rho_B} = \frac{1}{1 + (2/\pi - 1/3)y - p_D},$$
$$f_B = \frac{(2/\pi - 1/3)y - p_D}{1 + (2/\pi - 1/3)y - p_D}, \tag{11}$$

where

$$y \equiv R p_D \tag{12}$$

These fractions determine the equilibrium distribution of an ensemble of noninteracting tracers.

If $f_S \ll 1$, the tracer is predominantly found in the bulk. Since $p_D < 1$, Eq. (11) implies that this regime is possible only if $y \gg 1$; Eq. (12) then requires $R \gg 1$. The fractions of the residence time are $f_S \sim 1/y$ and $f_B \approx 1$. In these conditions, the diffusion coefficient is expected to be close to the free solution value D_0, with small corrections due to the adsorption events. These features are schematically represented in Fig. 5(a); an example of tracer trajectory in this regime was shown in Fig. 4(a).

The other limiting case, in which $f_B \ll 1$, is of dominant surface residence. From Eq. (11), this is possible only if $y \ll 1$ or, in terms of model parameters, $p_D \ll 1/R$. Since we typically work with $R \gg 1$, we have $y/\pi \gg p_D$ and Eq. (11) gives $f_B \sim y$, $f_S \approx 1$.

A balanced residence between bulk and surface is obtained for $y \sim 1$.

Dominant surface residence does not imply that the tracer displacement predominantly occurs in the surface because such displacement depends on the surface mobility. For instance, if the mobility on the surface is very low, it is possible that most hops are executed in the bulk, although the residence time is smaller there. This is schematically represented in Fig. 5(b), in which the tracer remains adsorbed for significant times but does not move along the solid walls; a trajectory corresponding to this regime was shown in Fig. 4(b) and does not have significant differences from that shown in Fig. 4(a). On the other hand, if the surface mobility is large, then the tracer can move along the solid walls before desorption, as illustrated in Fig. 5(c); this is a case in which residence and displacement are dominant at the surface. The trajectories consequently have pieces with rounded shape, as shown in Fig. 4(c).

We distinguish these regimes by comparing the surface and bulk displacements. In a time interval δt, the residence time in the bulk is $f_B \delta t$ and the residence time at the surface is $f_S \delta t$. The average displacements at the surface and in the bulk within this time are $\delta l_B \sim (D_0 f_B \delta t)^{1/2}$ and $\delta l_S \sim (D_S f_S \delta t)^{1/2}$, respectively, where D_0 and D_S are given in Eqs. (3) and (5). This leads to

$$\frac{\delta l_S}{\delta l_B} \sim \left[\frac{p_S}{p_D[(2/\pi - 1/3)R - 1]}\right]^{1/2} \sim \sqrt{\frac{p_S}{R p_D}}. \tag{13}$$

The second approximation in Eq. (13) considers $R \gg 1$ and omits a numerical factor of order 1. The corrections are proportional to $1/(2R)$; if R is not very large (e.g., between 10 and 50), these corrections may be relevant.

The scaling variable

$$x \equiv \frac{p_S}{Rp_D} \tag{14}$$

can be used to determine the region in which the diffusion length is larger. If $x \gg 1$, the mobility of the adsorbed tracers is sufficiently high so that the displacement along the surface is dominant; Fig. 4(c). If $x \ll 1$, the mobility in those surfaces is very low, so that the displacement in the bulk is dominant (even if the residence in the bulk is relatively short); Fig. 4(b).

The factor R that appears in Eqs. (12) and (14) is a consequence of Eq. (10). Thus, it represents a volume-to-area ratio which is scaled by the factor a (tracer diameter). The increase of this ratio means that the number of surface sites becomes smaller if compared with the number of bulk sites.

The diffusion coefficient is expected to be a function of the scaling variables x and y:

$$D = D_0 F(x, y), \tag{15}$$

where F is a dimensionless scaling function. For $y \gg 1$, which is the case of dominant bulk residence, we have $F(x, y) \sim 1$, independently of x. For $y \ll 1$, which is the case of dominant surface residence, two scenarios are possible:

(i) If $x \ll 1$, diffusion occurs mainly in the bulk, but the fraction of time in this region is $f_B \sim y$; thus,

$$D \sim yD_0 \tag{16}$$

and Eq. (15) gives $F(x, y) \sim y$.

(ii) If $x \gg 1$, diffusion occurs mainly in the surface, with the surface diffusion coefficient

$$D = D_S, \tag{17}$$

as given in Eq. (5); thus, $F(x, y) \sim p_S \sim xy$.

The relations for dominant surface residence also suggest

$$F(x, y) = yG(x), \quad y \ll 1, \tag{18}$$

where G is another scaling function: $G(x) \sim 1$ for $x \ll 1$ and $G(x) \sim x$ for $x \gg 1$.

Finally, note that the conditions $p_D < 1$ and $p_S < 1$ constrain the values of the scaling variables to

$$y < R, \quad xy < 1. \tag{19}$$

B. Numerical estimates

The diffusion coefficients are calculated from the $\log r_2 \times \log t$ plots by performing linear fits of the long-time data, as illustrated in Figs. 2(a) and 2(b). Here we focus on the case of dominant surface residence, $y \ll 1$, in which the diffusion coefficient may have significant deviations from the bulk value D_0. In terms of the model parameters, the scaling relations (15) and (18) suggest that $D/(Rp_D D_0)$ is a function of $p_S/(Rp_D)$; see also Eqs. (12) and (14).

Figure 6 shows that this scaling is observed with very good accuracy for a constant sphere radius $R = 10$; the universal curve in which the data collapse is $G(x)$ [Eq. (18)]. The inset of Fig. 6 shows the nonscaled data for several p_D and p_S. For $p_S/(Rp_D) \ll 1$, we have the regime of dominant bulk displacement, in which $D \sim Rp_D D_0$ [$G(x) \sim 1$]. In this case, the diffusion coefficient does not depend on the mobility of the tracer on the surface because it is very small. For

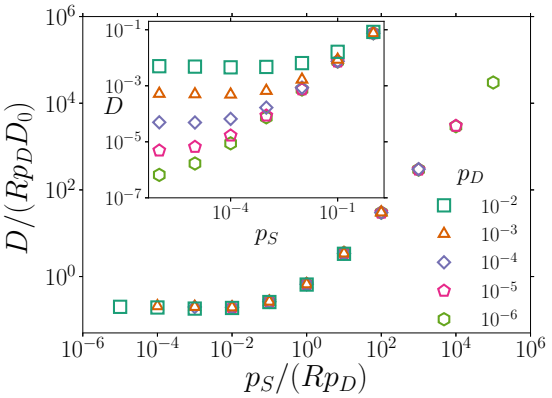

FIG. 6. Scaled diffusion coefficients as a function of a scaling variable for dominant surface residence, $R = 10$, and the probabilities indicated in the plot. The inset shows the diffusion coefficient as a function of p_S for each value of p_D.

$p_S/(Rp_D) \gg 1$, the data are in a curve with slope close to 1, which is consistent with $G(x) \sim x$ and $D \sim p_S D_0 = D_S$ [Eq. (5)]; this is the expected coefficient for dominant surface displacement.

Figure 7 shows $D/(Rp_D D_0)$ as a function of $p_S/(Rp_D)$ for several values of R and several values of the probabilities p_D and p_S. It confirms the validity of the scaling approach including the dependence of the diffusion coefficient on R. The data collapse is not so accurate as in with Fig. 6 because the finite values of R lead to corrections related to the approximation in Eq. (13).

C. Scaling relations with kinetic parameters

For an application of this model, the scaling variables must be related to the kinetic parameters defined in Sec. II B. Using Eqs. (3)–(6), (12), and (14), we can define the physically measurable variables corresponding to y and x, respectively, as

$$y_M \equiv \frac{adr_D}{D_0}, \quad x_M \equiv \frac{D_s}{adr_D} \tag{20}$$

(numerical factors were omitted when passing from x, y to x_M, y_M).

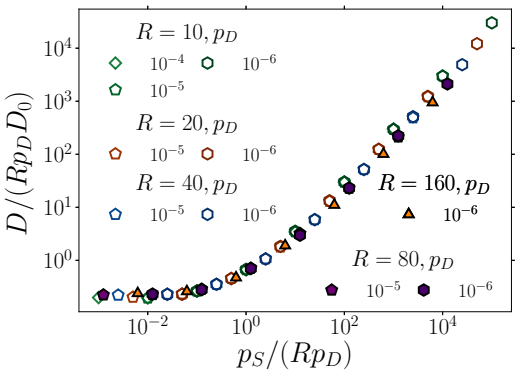

FIG. 7. Scaled diffusion coefficient as a function of a scaling variable in the regime of dominant surface residence, for the model parameters indicated in the plot.

The condition for dominant bulk residence, in which the diffusion coefficient is close to that in a free solution, is $y_M \gg 1$, which gives $r_D \gg D_0/(ad)$. This relation sets a minimum value for the desorption rate, which depends on the free diffusion properties and on geometric properties of the medium. When this rate is far below this limit, i.e., $r_D \ll D_0/(ad)$, dominant surface residence is observed.

The dominant surface residence and bulk displacement is observed for $x_M \ll 1$, which gives $D_s \ll adr_D$. On the other hand, if residence and displacement are dominant at the surface, we have $D_s \gg adr_D$.

V. ADSORPTION ISOTHERMS

The fractions of the residence time in the bulk and on the surface given in Eq. (11) are long-time averages, i.e., steady state properties of the single-particle diffusion model. Those fractions may be measured in the time ranges in which the diffusion coefficients are calculated; see, e.g., the linear fits in Figs. 2(a) and 2(b). Since the model obeys detailed balance conditions, an ensemble of noninteracting tracers in equilibrium will be distributed in bulk and surface regions with the same fractions f_B and f_S.

In such equilibrium condition, the surface coverage θ is defined as the number of adsorbed tracers per unit area of the surface, and the density of tracers in the bulk, σ, is defined as the number of tracers per unit volume of bulk sites. Let N be the number of tracers in a unit cell of the lattice, i.e., inside a cube of side $2aR$. The number of tracers in the bulk is $f_B N$ and the number of tracers on the surface is $f_S N$, where f_B and f_S are given in Eq. (11). Thus, the surface coverage and the bulk density for large R are

$$\theta = \frac{f_S N}{4\pi (aR)^2}, \quad \sigma = \frac{f_B N}{(2aR)^3 - 4\pi (aR)^3/3}. \tag{21}$$

Using Eq. (11), we obtain

$$\theta = \frac{1}{1 - [(2/\pi - 1/3)R]^{-1}} a {p_D}^{-1} \sigma. \tag{22}$$

This linear relation between θ and σ is a Henry isotherm.

For large spheres compared to the tracers ($R \gg 1$) and using the activated form of p_D in Eq. (7), we obtain

$$\theta = \frac{a}{p_D}\sigma = \frac{aR}{y}\sigma = a \exp[(E_B - E_S)/(k_B T)]\sigma. \tag{23}$$

This isotherm is expressed in terms of different quantities to help its physical interpretation.

In the last equality of Eq. (23), we have $E_S < E_B$. Thus, for fixed σ, we expect a decrease of θ as the temperature increases (favoring desorption).

The first equality in Eq. (23) involves two factors: the lattice constant a, which is a microscopic length characterizing the mean free path of the tracer, and the probability p_D, which is related to the strength of adsorption. In cases of strong adsorption, we have $p_D \ll 1$, so that a/p_D is much larger than the microscopic length a. Physically, it means that the fractional occupancy of surface sites is much larger than the fractional occupancy of bulk sites. This is reasonable for dominant surface residence.

The second equality in Eq. (23) involves a factor which is the ratio between the characteristic length of the porous medium, aR, and the scaling variable y. If that length is known, the adsorption isotherm may be used to distinguish regimes of dominant surface or bulk residence.

Some previous models of bulk and interface diffusion in the pores of impenetrable sphere packings considered the adsorption isotherm as part of the model definition (in contrast with our work, which postulates the values of the kinetic parameters p_S and p_D). In Ref. [5], the calculations considered the condition $K_{eq} \ll L_c$ to relate the equilibrium constant K_{eq} of the isotherm and a characteristic length scale L_c of the medium (see Eq. 4.33 of that paper). In the notation of the present model, we understand that these quantities are given as $K_{eq} \sim a/p_D$ and $L_c \sim aR$; consequently, that work had a focus on the case $y \gg 1$, which corresponds to dominant bulk residence. In Ref. [9], the isotherm was written in terms of two dimensionless quantities, the coverage θ and a relative humidity x, and the calculations were performed for $\theta/x \approx 4$. In the context of our model, we understand that this value of θ/x means that the occupancy fractions in bulk and interface are of the same order of magnitude; thus, the kinetic coefficients of mass transfer between them are also of the same order. Since diffusion in the bulk is faster, this is expected to be a regime of dominant bulk displacement.

VI. CROSSOVER TO NORMAL DIFFUSION

Here we extend the scaling approach of Sec. IV A to describe quantitatively the slowdown (or saturation) of tracer displacement that separates the initial regime and the asymptotic regime, as shown in Fig. 2. We focus on the case of dominant surface residence ($y \ll 1$).

For large sphere radius, the number of bulk sites is much larger than the number of surface sites. Due to the uniform initial tracer distribution, most tracers start moving in the bulk. At short times, the mean square displacement is not very different from the free solution value $\langle r^2 \rangle \sim D_0 t_D$ (the apparent anomaly in Fig. 3 is very weak). However, this initial regime ends when the tracers collide with solid walls, whose distance is of order Ra; thus, $\langle r^2 \rangle \sim (Ra)^2$ at this point. The characteristic time t_I in which it occurs is

$$t_I \sim \frac{(Ra)^2}{D_0} \sim R^2 \tau. \tag{24}$$

The crossover to the asymptotic normal diffusion is expected at a time t_c in which the long-time diffusion length is of the same order as the sphere radius $\mathcal{R} = Ra$. In this situation, the homogeneity of the medium begins to control the diffusion. If $t_c \gg t_I$, the mean square displacement is approximately constant between t_I and t_c.

In the regime of dominant bulk displacement ($x \ll 1$), D is given in Eq. (16) and the crossover time is denoted $t_c^{(B)}$. The diffusion length at that time is $\delta l_B \sim \sqrt{y D_0 t_c^{(B)}}$. This crossover occurs when $\delta l_B \sim Ra$, which gives

$$t_c^{(B)} \sim \frac{R}{p_D}\tau. \tag{25}$$

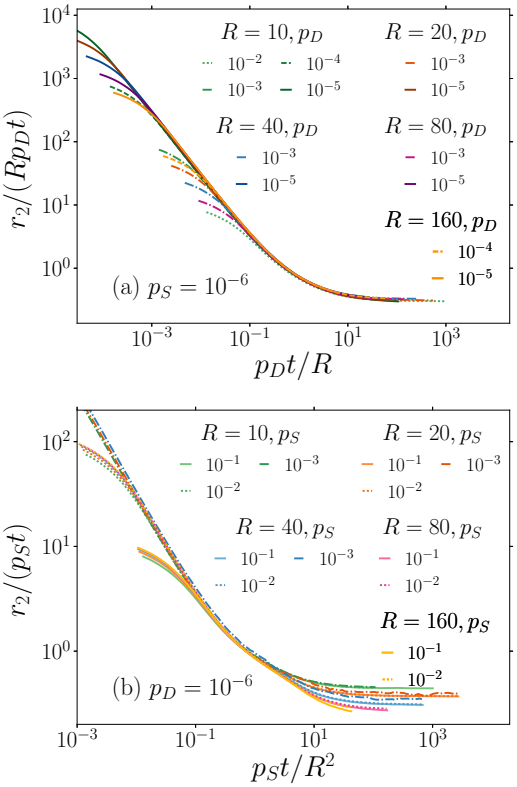

FIG. 8. Scaled mean square displacement as a function of scaled time in conditions of dominant surface residence and (a) dominant bulk displacement, (b) dominant surface displacement.

At longer times, the mean square displacement varies as $\langle r^2\rangle \sim yD_0t_D \sim Rp_DD_0t_D$. Thus, it is expected to follow the dynamic scaling relation

$$\langle r^2\rangle \sim Rp_DD_0t_D\mathcal{F}\left(\frac{t_D}{t_c^{(B)}}\right), \tag{26}$$

where $\mathcal{F}$ is a scaling function. This relation includes the regime of diffusion slowdown (but not the initial regime $t < t_1$).

Using Eqs. (2) and (3), we can write Eq. (26) in terms of dimensionless variables; it predicts that $r_2/(Rp_Dt)$ is a function of tp_D/R. Figure 8(a) shows a plot of those quantities for model parameters consistent with the conditions $y \ll 1$ and $x \ll 1$. The left parts of the curves correspond to short-time displacements, which are not described by the scaling approach. The saturation of r_2 corresponds to the inclined region, with slope close to -1, and the asymptotic normal diffusion corresponds to the horizontal region. In these two regions, the data collapse is very good.

Since r_2 is constant between t_A and $t_c^{(B)}$, the number of time decades of this regime is $\log_{10}[t_c^{(B)}/t_A] = \log_{10}(1/y)$ here, Eqs. (12), (25), and (24) were used. For instance, consider the data in Fig. 2(b), in which $\log_{10}(1/y) \approx 1.4$; for $p_S \leqslant 10^{-3}$ ($x \leqslant 2.5 \times 10^{-2}$), r_2 is approximately constant from $t \sim 10^3$ until a time slightly above 10^4, i.e., more than one time decade later.

In the case of dominant surface displacement ($x \gg 1$), the diffusion coefficient is given by Eq. (5) and the diffusion length at a crossover time $t_c^{(S)}$ is $\delta l_S \sim \sqrt{D_Sf_St_c^{(S)}}$. The crossover occurs when $\delta l_B \sim Ra$, so that

$$t_c^{(S)} \sim \frac{R^2}{p_S}\tau. \tag{27}$$

The long-time mean square displacement is $\langle r^2\rangle \sim p_SD_0t_D$; this leads to the dynamic scaling relation

$$\langle r^2\rangle \sim p_SD_0t_D\mathcal{G}\left(\frac{t_D}{t_c^{(S)}}\right), \tag{28}$$

where $\mathcal{G}$ is another scaling function.

In terms of dimensionless quantities, Eq. (28) predicts that $r_2/(p_St)$ is a function of tp_S/R^2. These scaled variables are plotted in Fig. 8(b) considering data with $x \gg 1$, $y \ll 1$. We observe a good data collapse in the inclined region, which corresponds to the saturation of r_2. There are deviations in the right parts of those plots, which correspond to normal diffusion.

These deviations are also consequence of the approximation in Eq. (13) and in the scaling variable of Eq. (14), which neglected corrections of order $1/R$. Also note that this is a regime in which most hops are executed along the surface walls and the hops between different spheres are possible only at the narrow bridges connecting them. Those bridges have a small number of sites [see, e.g., Fig. 1(a)], which means that they become proportionally narrower as R increases. In Fig. 8(b), this feature helps to explain the small decrease in the value of r_2/p_St as R increases.

Equations (27) and (24) give $t_c^{(S)}/t_A \sim 1/p_S$, which means that constant r_2 is observed in a number of time decades $\log_{10}(1/p_S)$. For instance, in Fig. 2(a), we have $\log_{10}(1/p_S) = 3$. Indeed, for $p_D \leqslant 10^{-5}$ ($y \leqslant 10^{-4}$, $x \geqslant 10$), r_2 is approximately constant from $t \sim 10^2$ to $t \sim 10^5$, i.e., in three time decades.

It is important to stress that the features described here are consequences of the choice of a uniform (nonequilibrium) initial distribution of the tracers. If the initial distribution of tracer positions is obtained after thermalization (i.e., after a time longer than $t_c^{(B)}$ or $t_c^{(S)}$), then we expect that the subsequent mean square displacement increases linearly in time since short times, with the same diffusion coefficient obtained in Sec. IV. This is illustrated in Fig. 9, in which the time counter was restarted after a thermalization time 10^6 and the displacements were measured from the tracers positions at the restart. For the same model parameters, Figure 2(a) shows the initial slow increase of r_2 and the subsequent slowdown up to times $\sim 10^5$ in the case of initial uniform distribution of tracer positions. This shows the importance of accounting for effects of initial conditions in the analysis of real diffusion problems.

If the crossover time $t_c^{(B)}$ [Eq. (25)] is experimentally measured, it can be used to estimate the desorption rate; on the other hand, if the adsorption isotherm is known [Eq. (23)], then the relaxation time to attain equilibration, $t_c^{(B)}$, can be predicted. Along the same lines, if the crossover time $t_c^{(S)}$ [Eq. (27)] is experimentally measured, it can be used to estimate the ratio of diffusion coefficients at the surface and in the bulk. A similar effect of initial conditions was observed in the model of Ref. [27], which suggested the measurement of

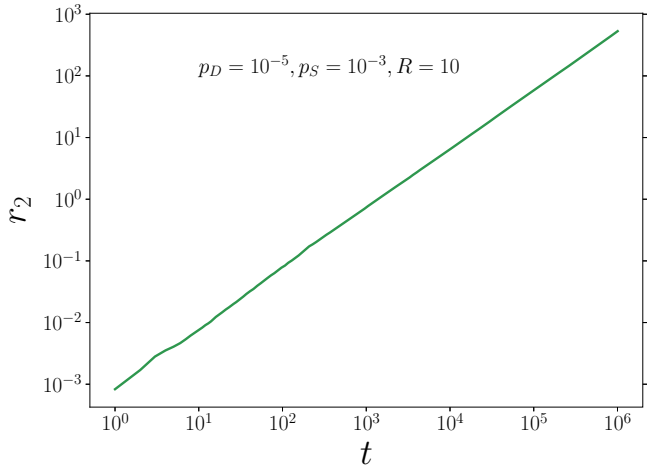

FIG. 9. Mean square displacement as a function of time for the parameter set shown in the plot, with times and displacements measured from the position of each tracer after a thermalization time 10^6.

a crossover time in the fluctuation of the diffusion coefficient for estimating the surface diffusivity.

A slowdown of the mean square displacement was also observed in diffusion of colloidal suspensions of hard spheres with excluded-volume interactions in Ref. [28]. The effect was explained by the predisposition of encounters of the spheres after they moved a distance close to their average separation and was modeled by a biased random walk. The slowdown is not so drastic as observed here, but an interesting aspect is that it is also related to the first collision of the tracer with some obstacle (in that case, another tracer).

VII. RELATION WITH OTHER WORKS

Some previous works showed important consequences of the interplay of adsorption and surface diffusion.

In a recent work on Knudsen diffusion in cylindrical pores, the beneficial effect of surface diffusion was shown, particularly for the molecules to cross ink-bottle pores [29]. The calculated effective diffusion coefficients was approximately constant for slow surface diffusion, but varied by several orders with increasing surface diffusion coefficient. This parallels the behavior observed in Figs. 6 and 7, which suggests that the model of Ref. [29] also has scaling regimes of dominant displacement in the bulk or on the surface.

The beneficial effect of surface diffusion was also anticipated in a study of random walks in fractal media [30]. When the hops along the solid walls were more probable than the hops from the walls to the inner parts of the pores, the exponent α [Eq. (9)] increased in comparison to the case with uniform probabilities. This occurred because the enhanced adsorption allowed the tracers to contour the large obstacles in shorter times.

In the case of dominant surface residence with dominant bulk displacement, we showed that D is proportional to the ratio R between solid sphere radius and tracer mean free path. This occurs because the fraction of surface sites, where motion is delayed, is inversely proportional to R (also note that dominant surface residence is possible only for $Rp_D \ll 1$). This size effect is a consequence of strong adsorption. On the other hand, in media where adsorption can be neglected, size effects are consequence of steric hindrance, i.e., the particles with sizes close to the sizes of the pores have smaller D [31–33]. The limiting case of hindrance effect is the subdiffusion in fractal media, which is related to the self-similarity of the obstacle distributions [1]. Thus, for the interpretation of data on diffusion in porous media, it is important to distinguish these two possible origins of size effects, namely strong adsorption or steric hindrance.

There are also works which account for surface diffusion but which are apparently in regimes of dominant bulk residence or displacement. In Ref. [9], gas diffusion was modeled in porous media formed with simple cubic arrays of solid spheres, and the effective diffusion coefficient was shown to increase with the surface diffusivity. As discussed in Sec. V, the model parameters considered in that work give dimensionless values of surface coverage and of gas density with the same order of magnitude, which suggests dominant bulk displacement. The diffusion coefficients in a similar porous medium were calculated in Ref. [5] by accounting for surface diffusion, which considered a regime equivalent to dominant bulk residence.

Here we only observe small deviations of the mean-square displacement from the linear behavior [Eq. (15)] at short times (apparent anomaly), but it is interesting to note that crossovers from well defined short-time anomalous scaling [Eq. (9)] to normal diffusion were already observed in other systems where adsorption plays a role. Some recent examples are one-dimensional diffusion with reversible adsorption at one site [34], diffusion between parallel plates with different adsorption properties [35], and infiltration of adsorbed tracers in a porous medium with depth decreasing available area [11].

A recent work on polystyrene particle diffusion in random packings of glass beads showed that normal and anomalous diffusion can be obtained with different solutions [8]. The porosity of those packings varied between 0.34 and 0.36, the particles had diameter 0.400 μm, and the beads had diameters between 5.4 and 30 μm. The diffusion in a glycerol/water mixture was normal, but anomalous diffusion with exponent $\alpha = 0.6$ was observed in a solution of semidilute hydrolyzed polyacrylamide (HPAM). In the anomalous case, the maximal measured mean square displacements were approximately one tenth of the square bead radius. Particle trajectories were monitored and, in HPAM solution, some of them had curvatures that indicated long times adsorbed in the bead surfaces.

Figure 4(c) shows a trajectory of a tracer particle whose rounded parts are very similar to those observed in Ref. [8]. This suggests a regime of dominant surface residence and displacement in that experiment. Our simulations also show a slow increase of the mean-square displacement at short times, but this is a consequence of the uniform initial distribution of tracers in the pores (most of them starting at the bulk), while the distribution in the experiments is probably closer to equilibrium. Moreover, the slopes α obtained here (Fig. 3) are much larger than the exponents obtained in the experiments, and our random walk model is Gaussian, while the experimental distributions of particle displacements were not

Gaussian. These observations preclude a quantitative description of those experiments with the present model.

VIII. CONCLUSION

We studied a model of random walks in the interstices of a simple cubic packing of solid spheres which represents diffusion of a tracer interacting with the internal surface of that medium. The diffusion in the solid walls and in the bulk fluid have different coefficients and hops from those walls to the bulk are less probable than hops in the opposite sense, which describes adsorption effects. Although the study was performed with a relatively simple pore-solid geometry, several experimental and theoretical works with this geometry justify that choice.

A scaling approach showed three different regimes for diffusion in this medium: dominant bulk residence, in which the tracer moves in the bulk most of the time and the diffusion coefficient is of the same order of the coefficient in free solution; dominant surface residence with dominant bulk displacement, in which the tracer is adsorbed on the sphere walls most of the time, but with a very small mobility in that region, so that the average displacement is dominated by hops in the bulk; and dominant surface residence with dominant surface displacement, in which the tracer is adsorbed on the sphere walls most of the time and executes most hops along those walls. These regimes are quantitatively characterized in terms of model probabilities and, for applications, they are related to the geometric properties of the medium, the diffusion coefficients, and the desorption rate. This scaling approach is confirmed by numerical simulations. The average residence times of tracers in the bulk and on the surface lead to a simple adsorption isotherm relating surface and bulk densities with kinetic parameters and the medium geometry.

In cases of strong adsorption and/or low mobility on the sphere surfaces, simulations with initially uniform tracer distributions suggest an apparent subdiffusion at very short times. The regime of dominant surface residence and dominant surface displacement also shows rounded trajectories of adsorbed particles. These features are qualitatively similar to those observed in the colloidal particle adsorption in the HPAM solution described in Ref. [8]. This shows that the scaling regimes analyzed here may be of relevance to experiments, although the quantitative description may require modeling more complex interactions.

We believe that the scaling relations obtained here may also be extended to diffusion in porous medium formed by packings of other solids with smooth shapes and with aspect ratios close to 1 (i.e.. characterized by a single length parameter). In those cases, typical values of the porosity are between 0.4 and 0.7 [36], which is of the same order as the porosity of our samples. We also believe that the present work motivates the development of similar approaches for gas transport when surface diffusion plays a role [29,37].

ACKNOWLEDGMENTS

C.O. acknowledges support from Brazilian agency CAPES (88882.151325/2017-01). F.D.A.A.R. acknowledges support from Brazilian agencies CNPq (304766/2014-3), FAPERJ (E-26/202941/2015), and CAPES (88881.068506/2014-01).

[1] D. ben Avraham and S. Havlin, *Diffusion and Reactions in Fractals and Disordered Systems* (Cambridge University Press, Cambridge, UK, 2000).
[2] J. P. Bouchaud and A. Georges, Phys. Rep. **195**, 127 (1990).
[3] I. C. Kim and S. Torquato, J. Appl. Phys. **69**, 2280 (1991).
[4] I. C. Kim and S. Torquato, J. Chem. Phys. **96**, 1498 (1992).
[5] J. A. Ochoa-Tapia, J. A. del Rio P., and S. Whitaker, Chem. Eng. Sci. **48**, 2061 (1993).
[6] S. G. J. M. Kluijtmans and A. P. Philipse, Langmuir **15**, 1896 (1999).
[7] H. Liasneuski, D. Hlushkou, S. Khirevich, A. Holtzel, U. Tallarek, and S. Torquato, J. Appl. Phys. **116**, 034904 (2014).
[8] F. Babayekhorasani, D. E. Dunstan, R. Krishnamoorti, and J. C. Conrad, Soft Matter **12**, 8407 (2016).
[9] M. Mirbagheri and R. J. Hill, Chem. Eng. Sci. **160**, 419 (2017).
[10] M. Roding, Phys. Rev. E **98**, 052908 (2018).
[11] F. D. A. Aarão Reis and D. di Caprio, Phys. Rev. E **89**, 062126 (2014).
[12] S. P. Thampi, S. Ansumali, R. Adhikari, and S. Succi, J. Comput. Phys. **234**, 1 (2013).
[13] M. J. Skaug and D. K. Schwartz, Ind. Eng. Chem. Res. **54**, 4414 (2015).
[14] S. Eloul, E. Kätelhön, and R. G. Compton, Phys. Chem. Chem. Phys. **18**, 26539 (2016).
[15] X. Yang, C. Liu, Y. Li, F. Marchesoni, P. Hänggif, and H. P. Zhang, Proc. Natl. Acad. Sci. USA **114**, 9564 (2014).
[16] V. Privman, Colloids Surf. A **165**, 231 (2000).
[17] Z. Adamczyk, Curr. Opin. Colloid Interface Sci. **17**, 173 (2012).
[18] N. Kleppmann, F. Schreiber, and S. H. L. Klapp, Phys. Rev. E **95**, 020801(R) (2017).
[19] F. D. A. Aarão Reis and R. B. Stinchcombe, Phys. Rev. E **70**, 036109 (2004).
[20] T. J. Oliveira and F. D. A. Aarão Reis, Phys. Rev. B **87**, 235430 (2013).
[21] A. Rai, M. Warrier, and R. Schneider, Comput. Mater. Sci. **46**, 469 (2009).
[22] R. Metzler, J.-H. Jeon, A. G. Cherstvya, and E. Barkai, Phys. Chem. Chem. Phys. **16**, 24128 (2014).
[23] F. A. Oliveira, R. M. S. Ferreira, L. C. Lapas, and M. H. Vainstein, Front. Phys. **7**, 18 (2019).
[24] D. S. Dean and G. Oshanin, Phys. Rev. E **90**, 022112 (2014).
[25] N. Alcázar-Cano and R. Delgado-Buscalioni, Soft Matter **14**, 9937 (2018).
[26] Y. Li, O. Kahraman, and C. A. Haselwandter, Phys. Rev. E **96**, 032139 (2017).
[27] T. Akimoto and K. Seki, Phys. Rev. E **92**, 022114 (2015).
[28] W. van Megen, Phys. Rev. E **73**, 011401 (2006).
[29] T. Hori, T. Kamino, Y. Yoshimoto, S. Takagi, and I. Kinefuchi, Phys. Rev. E **97**, 013101 (2018).
[30] F. D. A. A. Reis, J. Chem. Phys. **111**, 310 (1999).

[31] R. Raccis, A. Nikoubashman, M. Retsch, U. Jonas, K. Koynov, H.-J. Butt, C. N. Likos, and G. Fytas, ACS Nano **5**, 4607 (2011).

[32] D. Hlushkou, A. Svidrytski, and U. Tallarek, J. Phys. Chem. C **121**, 8416 (2017).

[33] S.-J. Reich, A. Svidrytski, A. Holtzel, J. Florek, F. Kleitz, W. Wang, C. Kubel, D. Hlushkou, and U. Tallarek, J. Phys. Chem. C **122**, 12350 (2018).

[34] G. Dumazer, E. Flekkoy, F. Renard, and L. Angheluta, Phys. Rev. E **96**, 042106 (2017).

[35] V. G. Guimarães, H. V. Ribeiro, Q. Li, L. R. Evangelista, E. K. Lenzi, and R. S. Zola, Soft Matter **11**, 1658 (2015).

[36] D. Coelho, J.-F. Thovert, and P. M. Adler, Phys. Rev. E **55**, 1959 (1997).

[37] K. Wu, X. Li, C. Wang, W. Yu, and Z. Chen, Ind. Eng. Chem. Res. **54**, 3225 (2015).